Chinese Chemical Letters 37 (2026) 111168

Contents lists available at ScienceDirect

Chinese Chemical Letters

journal homepage: www.elsevier.com/locate/cclet

3D fractal expanding of a Sierpiński triangular-faced supramolecular cage for enhanced photocatalytic performance

Zhilong Jiang[a,1], Qiaolin Chen[a,1], Min Wang[a], Fengxue Liu[b], Xiaojie Huang[a], Bangtang Chen[a], Qiangqiang Dong[b], Mingzhao Chen[a], Yifan Lin[c,*], Pingshan Wang[a,b,**], Jun Wang[a,*]

[a] *Institute of Environmental Research at Greater Bay Area, Key Laboratory for Water Quality and Conservation of the Pearl River Delta, Ministry of Education, Guangzhou University, Guangzhou 510006, China*
[b] *Hunan Key Laboratory of Micro & Nano Materials Interface Science, College of Chemistry and Chemical Engineering, Central South University, Changsha 410083, China*
[c] *College of Light Chemical Industry and Materials Engineering, Shunde Polytechnic, Foshan 528300, China*

ARTICLE INFO

Article history:
Received 15 January 2025
Revised 23 March 2025
Accepted 1 April 2025
Available online 1 April 2025

Keywords:
Fractal-expansion
Metallo-organic ligands
Sierpiński triangles
Triangular prisms
Photocatalysis

ABSTRACT

Fractal assembly in discrete structures, especially for artificial supramolecular species, has attracted significantly increased interest over the past two decades. In this study, we present the precisely controlled fractal expanding synthesis of a novel triangular prism supramolecule featuring Sierpiński triangular face, which was achieved through a module-intervened self-expansion strategy. The homoleptic **S1** was firstly synthesized through the assembly of ligand **L1** with Zn^{2+} ions. Based on the triangular-faced prism **S1**, we further introduced Sierpiński triangular faces on the section of the heteroleptic supramolecular cage **S2** with an expanded inner cavity and more abundant active sites for photocatalytic properties. The topotactic architectures for both **S1** and **S2** were fully characterized by nuclear magnetic resonance spectroscopy, high-resolution electrospray ionization mass spectrometry, transmission electron microscopy, and atomic force microscopy. Furthermore, the enhanced photocatalytic activity of the fractal expanded **S2** was performed *via* the superior amine oxidative efficiency over **S1**. This study proposes the unprecedented fractal expanding strategy for three-dimensional supramolecular species with higher complexity, potentially opening new avenues for structural regulation of artificial fractal molecules.

© 2025 Published by Elsevier B.V. on behalf of Chinese Chemical Society and Institute of Materia Medica, Chinese Academy of Medical Sciences.

Fractals are patterns that repeat at different scales, with smaller parts mirroring the larger whole [1]. These geometries are intriguing due to their profound implications in the domains of aesthetics, mathematics, and philosophy [2,3]. Nature is abundant with examples of fractal shapes, including the Koch snowflake, the branching structure of trees, the striking branching of lightning, the complex network of the human nervous system, and the rugged landscapes of mountains. As a celebrated fractal geometry, Sierpiński triangle, which was first introduced by the Polish mathematician Waclaw Sierpiński [4], has recently captured the attention of the synthesis chemistry community. This fractal has been the subject of numerous two-dimensional (2D) molecule syntheses, and was driven by advancements in on-surface synthesis and solution-state supramolecular self-assembly techniques [5–9]. However, the exploration of Sierpiński triangle in three-dimensional (3D) geometric configurations poses a significant challenge in the field of synthetic chemistry, especially in the context of geometric modeling and fractal geometry.

Coordination-driven self-assembly, which is a versatile synthetic method playing vital role in synthetic chemistry region, has been widely used for constructing nano geometric structure with characteristic regularity and elegance [10,11]. In the past twenty years, a great amount of novel 3D architectures such as prisms, helicates, polyhedra, spheroids, interlocked structures, barrels have been reported by Stang [12–15], Fujita [16–20], Nitschke [21–27], Clever [28–31], Newkome [32–35], and many others [36–45]. Among the coordination-driven constructs, 3D geometric supramolecules exhibiting Sierpiński fractal topologies are esteemed for their aesthetic appeal. Newkome's group has success-

* Corresponding authors.
** Corresponding author at: Hunan Key Laboratory of Micro & Nano Materials Interface Science, College of Chemistry and Chemical Engineering, Central South University, Changsha 410083, China.
E-mail addresses: 24011@sdpt.edu.cn (Y. Lin), chemwps@csu.edu.cn (P. Wang), wangjun@gzhu.edu.cn (J. Wang).
[1] These authors are contributed equally to this work.

https://doi.org/10.1016/j.cclet.2025.111168
1001-8417/© 2025 Published by Elsevier B.V. on behalf of Chinese Chemical Society and Institute of Materia Medica, Chinese Academy of Medical Sciences.

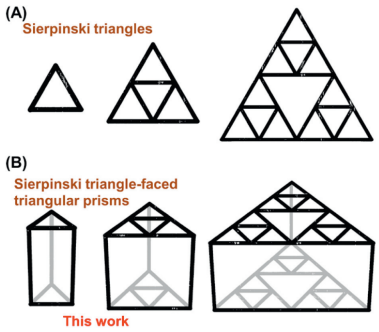


Fig. 1. Schematic illustration of (A) the Sierpiński triangles and (B) the Sierpiński triangle-faced triangular prisms.

fully demonstrated a megastructural Sierpiński pyramid through the stacking of Sierpiński triangles, achieving molecular-directed intertwinement of the alkyl side chains through a second-order assembly process [46]. Wang's group has unveiled the fabrication of Sierpiński tetrahedrons and octahedrons, which were constructed through a meticulous process with the utilization of a truncated Sierpiński triangular kernel as face ligand, complementary bridge-shaped ligands as vertexes, and Zn^{2+} or Cd^{2+} ions as pivotal connectors [47]. Although individual speices featuring fractal characteristics have been developed, controllable methods that producing giant fractal architectures with higher complexity from prototypical artificial supramolecules are still difficult to be realized.

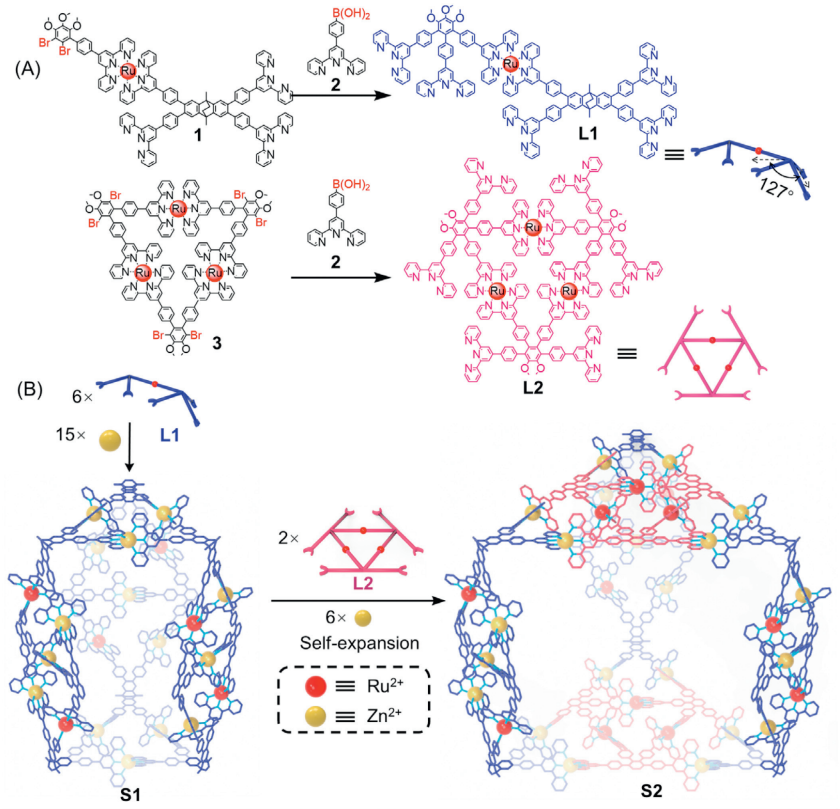
Terpyridine (tpy) based ligands exhibit exceptional self-assembly properties and are pivotal in the field of aesthetic giant supramolecular constructions [48–57]. Particularly, the coordination between terpyridine and Ru^{2+} ions exhibit remarkably stability even under extreme chemical conditions, which have been well documented as promising connectors for innovative supramolecular structure (Fig. 1) [58–62]. In this study, we present the synthesis of a novel triangular prism supramolecule **S1** characterizing by triangular faces and rhombus edges, which is formed through the self-assembly of penta-topic metal-organic ligand **L1** with Zn^{2+} ions. The **S1** provides an internal cavity with large windows and functionalized interior environment for the accommodation of small molecules, showing great potential in catalytic applications. With the introduction of a metallo-organic modular ligand **L2**, the architecture of **S1** could be converted into an analogous framework **S2** *via* the topotactic Sierpiński triangular expanding on the opposite surfaces of the prism (Scheme 1). The architectures of **S1** and **S2** was characterized through various analytical techniques such as nuclear magnetic resonance spectroscopy (^{1}H NMR, 2D COSY, 2D NOESY, 2D DOSY), high-resolution electrospray ionization mass spectrometry (ESI-MS, ESI-TWIM-MS), transmission electron microscopy (TEM), and atomic force microscopy (AFM), as well as computer-generated modeling. To our knowledge, this is the first-example of triangular prism architecture with a Sierpiński fractal surface.

The pivotal metallo-organic ligand (MOL) **L1** was synthesized through a step-wise strategy involving a two-fold Suzuki-coupling reaction of precursor **1** with 4′-boronatopenyl [2,2′:6′,2′']terpyridine **2**. The ligand **L1** is composed of a tetra-terpyridine bridge-shaped ligand and a 1,2,3-tri-terpyridine ligand, connected by a Ru^{2+} ion. It features a V-shaped bis-terpyridine site and a serrated tri-terpyridine site, with a spatial angle of 127° [34]. As shown in Fig. 2A, two clean singlet peaks were observed at 9.44 and 9.42 ppm in a 1:1 ratio attributed to Ru^{2+} connected tpy-$H^{3',5'}$ protons, in addition, three clean singlets with integration ratio of 1:1:1 was observed in the non-aromatic region at 4.07, 3.75, and 3.74 ppm belong three methoxy groups, denoting the high purity of ligand **L1**. All the other signal peaks were assigned with the assistance of homonuclear chemical shift correlation spectroscopy (COSY) and nuclear overhauser effect spectroscopy (NOESY) experiments (Figs. S18 and S19 in Supporting information). To ascertain the molecular structure of the ligand **L1**, electrospray ionization mass spectrometry (ESI-MS) was further conducted. The ESI-MS spectrum of **L1** displayed a clean signal peak at *m/z* 1328.16 correlating to charge state 2+ caused by the loss of NTf_2^- anions, proving the successful synthesis of target ligand (Fig. S48 in Supporting information).

The triangular prism **S1** was assembled by mixing MOL ligand **L1** with $Zn(NO_3)_2{\cdot}6H_2O$ in a precise stoichiometric ratio of 2:5 in the mixed solvent of MeCN/MeOH (v/v, 3/1), and then refluxing at 85 °C for 8 h. After cooling to environmental temperature, an excessive methanol-saturated solution of $LiNTf_2$ salts was added to exchange counterpart anions, following by the filtration of red precipitate. The as-synthesized product was then identified by NMR and MS analyses. As shown in Fig. 2B, the ^{1}H NMR spectrum of **S1** exhibted a series of well-split signal peaks in the aromatic region. It could be observed that all signals of tpy-$H^{6,6''}$ protons on the uncoordinated sites of terpyridines shifted upfield (indicated by dashed line) due to the electron shielding effects of the metal ions, indicating the successful combination of **L1** with Zn^{2+} ions. Additionally, two singlets and one overlapping signal at 8.96, 8.94, and 8.90 ppm in a 1:4:1 ratio were attributed to six types of characteristic tpy-$H^{3',5'}$ protons, whereas the remaining tpy-$H^{3',5'}$ protons were overlapped in the 8.67–8.66 ppm region. In the non-aromatic region, signal peaks exhibited similar patterns to the uncoordinated **L1** ligands. Three singlets at 4.12, 3.82, and 3.81 ppm in a 1:1:1 integration ratio were attributed to three methoxy groups, indicating the formation of a highly symmetric product. Other assignments were fully confirmed by 2D COSY and 2D NOESY analyses (Figs. S37 and S38 in Supporting information).

ESI-MS and TWIM-MS analyses were performed to ensure the composition and purity of triangular prism **S1**. As shown in Fig. 2D, a series of peaks with successive charge states from 20+ to 10+ were observed at *m/z* 1151.79, 1227.16, 1310.90, 1404.49, 1509.78, 1629.11, 1765.48, 1922.84, 2106.42, 2323.38, and 2583.74 owing to the loss of different numbers of NTf_2^- anions during the ionization. The molecular weight was determined to be 28,638 Da, which fully matched the simulated values of $[(Zn_{15}L1_6)\ (NTf_2^-)_{42}]$ (Fig. 2C). Due to the large molecular weight of the assembled supramolecule and limitations in instrument resolution, the isotopic distribution of each charge might not be obtained. Furthermore, the TWIM-MS spectrum of **S1** (Fig. 2E) displayed a series of narrow drift time distributions for charge states from 17+ to 11+ with no plots of oligomer and isomeric structures, indicating the purity of target triangular prism **S1** and the absence of other assembly structures.

During the self-assembly process of triangular prism **S1**, the V-shaped bis-terpyridine moiety of ligand **L1** formed a triangular structure after combining with the metal ion Zn^{2+}, while the serrated tri-terpyridine moiety formed a diamond-shaped structure with intermediate bridging. To expand the faces of triangular prism **S1** into Sierpiński triangles, a metallo-organic modular ligand **L2** was designed. The **L2** features clip-shaped coordination units and rigid skeleton, which could complementally assemble with the V-shaped bis-terpyridine unit of **L1**, and the resulting assembly was preliminarily characterized by NMR and MS analysis (Fig. 3). The synthesis route of **L2** was provided in Scheme S2 (Supporting information). The ^{1}H NMR spectrum (Fig. 3C) of **L2** exhibited a series of clean signal peaks, indicating high purity and symmetry. Upon the addition of 2 equiv. ligand **L2** and 6 equiv. of Zn^{2+} ions into the assembled triangular prism **S1** solution, the mixture was subjected to reflux for 12 h. A red solid product was then isolated, yielding near quantitative efficiency. As shown in Fig. 3B, the ^{1}H NMR spectrum of this assembly product displayed three singlets and one overlapped signal peak at 8.91, 8.87–8.85, and 8.80 ppm



Scheme 1. The synthesis routs of (A) metallo-organic ligands **L1** and **L2**. (B) Self-assembly of triangular prism **S1** and expanded Sierpiński triangle-faced triangular prism **S2**.

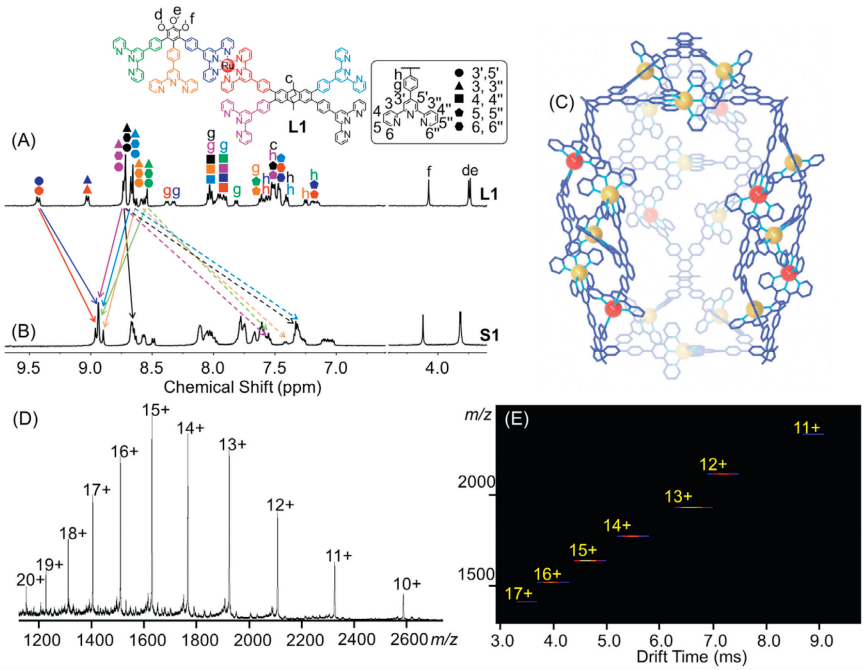


Fig. 2. ^{1}H NMR spectra (500 MHz, 298 K) of (A) **L1** in CD_3CN and (B) **S1** in CD_3CN. (C) Simulated structure of **S1**. (D) ESI-MS spectrum and (E) TWIM-MS plot of **S1**.

in a 1:5:1 ratio, which could be attributed to the seven kinds of tpy-H$^{3',5'}$ protons. The other two tpy-H$^{3',5'}$ protons were attributed to the overlapping peak at 8.08–7.92 ppm. In the non-aromatic region, two singlets and one overlapping signal peak were assigned to methoxy groups in an integral ratio of 1:2:2, indicating the successful assembly of triangular prism **S1** and ligand **L2** in a ratio of 1:2, as well as high symmetry of the product. All other assignments were confirmed by 2D COSY and 2D NOESY analyses (Figs. S41 and S42 in Supporting information).

The ESI-MS spectrum of supramolecule **S2** was shown in Fig. 3E, which displayed a series of signal peaks with successive charge states from 25+ to 13+ due to the loss of different numbers of NTf_2^- anions during the ionization. The calculated molecular weight of 45,592 Da exactly matched the designed structure with

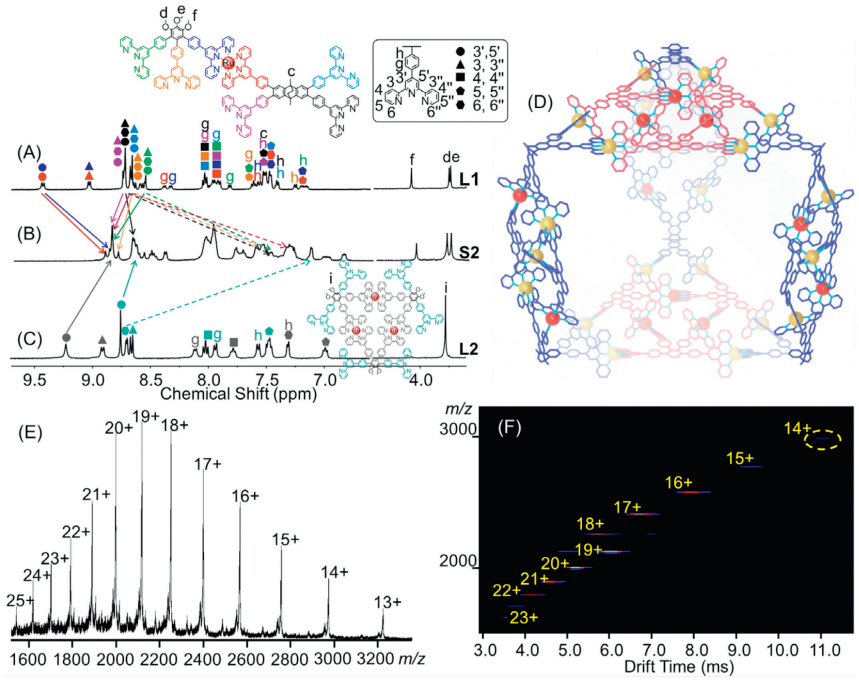


Fig. 3. ^{1}H NMR spectra (500 MHz, 298 K) of (A) **L1** in CD_3CN, (B) **S2** in CD_3CN, and (C) **L2** in DMSO–d_6. (D) Simulated structure of **S2**. (E) ESI-MS spectrum and (F) TWIM-MS plot of **S2**.

the formula of $[(Zn_{21}L1_6L2_2)\ (NTf_2^-)_{66}]$ (Fig. 3D), suggesting the formation of the Sierpiński triangle-faced triangular prism **S2**. The TWIM-MS spectrum (Fig. 3F) of **S2** displayed a series of narrow drift time distributions for charge states from 23+ to 14+ with no plots of oligomer and isomeric structures, further proving the successfully reassembly of triangular prism **S1** and ligand **L2** towards the Sierpiński triangle-faced triangular prism **S2** without other by-products.

To investigate the stability of triangular prisms **S1** and **S2**, gradient tandem mass spectrometry (gMS^2) experiments was conducted by isolating the charged ion [63]. The gMS^2 was carried out by isolating **S1** at *m/z* 1629.11 (15+) and **S2** at *m/z* 1999.46 (20+) with a graduated increase of the collision energy. As shown in Figs. S51 and S59 (Supporting information), **S1** and **S2** were completely dissociated at 50 V and 70 V respectively, indicating superior stability of the expanded structure. This may be attributed to the reduced molecular tension within the triangular prism introduced by the addition of the modular ligand **L2**, leading to the reassembly from prototypical triangular-faced **S1** towards Sierpiński triangular-faced **S2**.

To give an insight to the detail size and height information of **S1** and **S2**, DOSY NMR, transmission electron microscopy (TEM) and atomic force microscopy (AFM) were further conducted. As shown in Fig. 4, the DOSY experiments showed distinct bands at $\log D = -9.80$ ($D = 1.58 \times 10^{-10}\ m^2/s$) and -9.96 ($D = 1.10 \times 10^{-10}\ m^2/s$) for **S1** and **S2**, respectively. This demonstrates the formation of sole and discrete species in solution. The TEM samples were prepared by drop-casting of uniformly dispersed **S1** and **S2** (in MeCN at a concentration of $\sim 10^{-6}$) on a super thin-carbon film-coated grid (Cu, 300 mesh). As shown in Figs. 5A and F, the TEM images of **S1** and **S2** revealed individual particles with an averaged measured diameter of 5.0 ± 0.2, and 6.2 ± 0.2 nm, which were comparable to the geometry-optimized structure of **S1** (Figs. 5B and C) and **S2** (Figs. 5G and H). In the AFM images of **S1** (Figs. 5D and E), a series of dots with height within a certain range (4.6–5.2 nm) were observed on the mica surface, which were in accordance with the different placement forms of **S1**. AFM images of **S2** (Figs. 5I and J) show a series of dots with heights narrowly distributed between 5.1 nm and 5.2 nm on the mica surface, corresponding to the height of the simulated structure of triangular prism **S2**.

The as-synthesized triangular prisms **S1** and **S2** featuring huge cavities, open windows, and uniformly distributed active metal ions, suggesting great potential applications in molecular catalytic field. Imines are pivotal chemical compounds playing a crucial role in a variety of scientific and industrial domains [64,65]. A promising approach for imine synthesis involves photocatalytic selective oxidative coupling of amines. The photocatalytic reaction was conducted in an NMR tube, illuminated by a Xe lamp ($\lambda > 420$ nm, 300 W), using CD_3CN as the solvent, benzylamine as the substrate, and tert–butyl hydroperoxide (TBHP) as the oxidant. The progress of the photocatalytic reaction was monitored using NMR spectroscopy. As shown in Fig. 6, triangular prism **S1** (the molar ratio to benzylamine and TBHP is 1:500:2500) demonstrated remarkable photocatalytic activity, achieving a 98% conversion rate (with a yield of 95% after isolation) of benzylamine into *N*-benzylidine-1-phenylmethanamine within 60 min of exposure to light. In comparison, the larger fractal structure of Sierpiński triangle-faced triangular prism **S2**, exhibited suprior photocatalytic performance with 98% conversion rate (with a yield of 94% after isolation) of benzy-

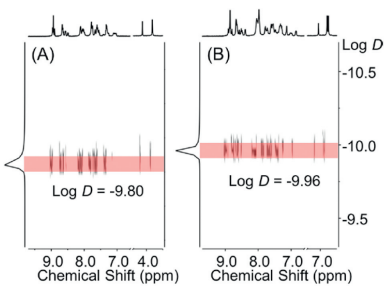


Fig. 4. DOSY spectra (500 MHz, 298 K) of (A) **S1** and (B) **S2** in CD_3CN.

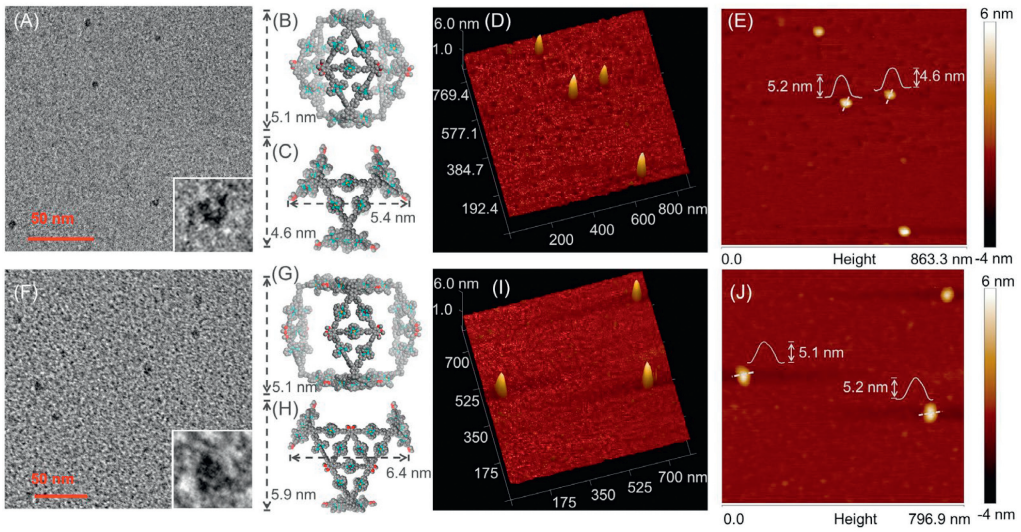


Fig. 5. TEM images of (A) **S1** and (F) **S2**. Representative energy-minimized structures from molecular model of (B), (C) **S1** and (G), (H) **S2**. 3D AFM images of (D) **S1** and (I) **S2**. AFM images of (E) **S1** and (J) **S2**.

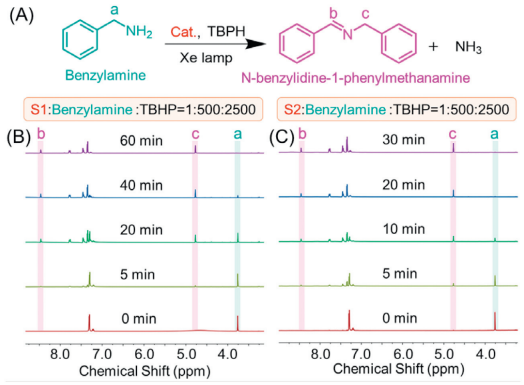


Fig. 6. (A) Schematic representation of the catalytic oxidation process of benzylamines to form *N*-benzylidine-1-phenylmethanamine. ^{1}H NMR spectra (500 MHz, 298 K, CD_3CN) of the benzylamine photocatalytic oxidation reaction of catalyzed by (B) **S1** and (C) **S2**, respectively.

lamine to the same product in only 30 min. The photocatalytic efficiency of ligands **L1** and **L2** was also examined, which performed ultra slower reaction rate within 200 and 300 min (Figs. S69 and S71 in Supporting information), respectively. The enhanced catalytic performace of **S2** might be attributed to the larger inner cavity for higher local concertration of the substrates and more active sites in the fractal expanded Sierpiński triangular faces, which facilitate the contact between the catalysts and small molecules and accelerate the catalaytic process. Furthermore, the substrate expansion experiments were further conducted by using supramolecule **S2** as catalyst under the same conditions (Figs. S73-S79 in Supporting information). Triangular prism **S2** exhibits excellent catalytic performances with various substrates, resulting in high efficiency with either electron donating or withdrawing substitution groups.

To further investigation the reaction mechanism for the oxidation of amine to imine, electron paramagnetic resonance (EPR) studies were conducted to detected singlet oxygen ($^1O_2$) in the presence of triangular prisms and 2,2,6,6-tetramethylpiperidine (TMPD) complex under visible-light irradiation in the CH_3CN solvent. As illustrated in Fig. S62 (Supporting information), the exposure of prisms **S1** and **S2** to 365 nm light resulted in the detection of a series of 1:1:1 triplet peak, indicating the presence of $^1O_2$. In the absence of light, no signals indicative of $^1O_2$ were detected. Additionally, the superoxide radical anion ($O_2^{\cdot-}$) was further tested. As shown in Fig. S63 (Supporting information), in the presence of $O_2^{\cdot-}$ trapping agent 5,5-dimethyl-1-pyrroline *N*-oxide (DMPO), the absorption signals of the DMPO–$O_2^{\cdot-}$ adduct were observed for **S1** and **S2** under visible-light irradiation. These results indicated the promising photo-oxidational applications of these metallo-organic cages. According to the above analyses and literature reports [66–69], we proposed the possible reaction mechanism for this photocatalytic benzylamine oxidation (Fig. S64 in Supporting information).

In summary, we have successfully synthesized the 3D Sierpiński triangle-faced triangular prism by introducing a modular ligand into a prototypical triangular prism system *via* a fractal expanding strategy. Both triangular prisms **S1** and **S2** featured large cavities and high stabilities by using pre-designed metallo-organic ligands. NMR, ESI-MS, TWIM-MS, TEM, and AFM, and molecular modelling were used to determine the architecture of the supramolecules. Photocatalytic performances suggested that the expanded inner cavity and higher density of the surface exposed active sites might lead to more favorable photo-oxidative process. The efficient generation of $^1O_2$ and $O_2^{\cdot-}$ determined by the EPR spectra figured out the possible mechanism of the photooxidation procedure, indicating great potential applications on functional photocatalytic materials. This work proposed a novel approach towards the fractal expanding of 3D metallo-organic cages, paving a new way for the controllable activity enhancement of artificial supramolecules with higher complexity.

Declaration of competing interest

The authors declare that they have no known competing financial interests or personal relationships that could have appeared to influence the work reported in this paper.

CRediT authorship contribution statement

Zhilong Jiang: Writing – review & editing, Validation, Supervision, Formal analysis, Data curation, Conceptualization. **Qiaolin Chen:** Methodology, Investigation, Formal analysis, Data curation. **Min Wang:** Writing – original draft, Data curation. **Fengxue Liu:** Data curation. **Xiaojie Huang:** Data curation. **Bangtang Chen:** Data curation. **Qiangqiang Dong:** Data curation. **Mingzhao Chen:** Investigation, Funding acquisition, Data curation. **Yifan Lin:** Writing –

review & editing, Writing – original draft, Funding acquisition, Conceptualization. **Pingshan Wang:** Writing – review & editing, Funding acquisition, Conceptualization. **Jun Wang:** Writing – original draft, Investigation, Data curation.

Acknowledgments

This research was supported by the Major Science and Technology Projects of Yunnan Province (No. 202302AB080016); the National Natural Science Foundation of China (Nos. 22101060, 22371056, and 52303269); the Science and Technology Research Project of Guangzhou (Nos. 202201020201 and 2023A03J0624).

Supplementary materials

Supplementary material associated with this article can be found, in the online version, at doi:10.1016/j.cclet.2025.111168.

References

[1] J.W. Cannon, Amer. Math. Monthly 91 (1984) 594–598.
[2] A. Rieger, Philos. Math. 26 (2017) 234–250.
[3] J. Liu, Comp. Cont. Philos. 14 (2022) 315–317.
[4] C.A. Reiter, Comput. Graph. 18 (1994) 885–891.
[5] R. Canyellas, C. Liu, R. Arouca, et al., Nat. Phys. 20 (2024) 1421–1428.
[6] J. Dai, X. Zhao, Z. Peng, et al., J. Am. Chem. Soc. 145 (2023) 13531–13536.
[7] Z. Jiang, Y. Li, M. Wang, et al., Angew. Chem. Int. Ed. 56 (2017) 11450–11455.
[8] Z. Jiang, D. Liu, M. Chen, et al., iScience 23 (2020) 101064.
[9] N. Li, X. Zhang, G.C. Gu, et al., Chin. Chem. Lett. 26 (2015) 1198–1202.
[10] Y. Sun, C. Chen, J. Liu, et al., Chem. Soc. Rev. 49 (2020) 3889–3919.
[11] E.G. Percástegui, V. Jancik, Coord. Chem. Rev. 407 (2020) 213165.
[12] Y. Li, S.S. Rajasree, G.Y. Lee, et al., J. Am. Chem. Soc. 143 (2021) 2908–2919.
[13] X. Yan, P. Wei, Y. Liu, et al., J. Am. Chem. Soc. 141 (2019) 9673–9679.
[14] H. Zhu, Q. Li, B. Shi, et al., Angew. Chem. Int. Ed. 59 (2020) 20208–20214.
[15] Y. Ye, T.R. Cook, S.P. Wang, et al., J. Am. Chem. Soc. 137 (2015) 11896–11899.
[16] K. Iizuka, H. Takezawa, M. Fujita, J. Am. Chem. Soc. 146 (2024) 32311–32316.
[17] Y. Domoto, M. Abe, G.R. Genov, et al., Angew. Chem. Int. Ed. 62 (2023) e202303714.
[18] Y. Domoto, M. Abe, M. Fujita, J. Am. Chem. Soc. 143 (2021) 8578–8582.
[19] D. Fujita, Y. Ueda, S. Sato, et al., Nature 540 (2016) 563–566.
[20] Y. Domoto, M. Abe, T. Kikuchi, et al., Angew. Chem. Int. Ed. 59 (2020) 3450–3454.
[21] J.A. Davies, T.K. Ronson, J.R. Nitschke, J. Am. Chem. Soc. 146 (2024) 5215–5223.
[22] H.K. Liu, T.K. Ronson, K. Wu, et al., J. Am. Chem. Soc. 145 (2023) 15990–15996.
[23] C.F. Espinosa, T.K. Ronson, J.R. Nitschke, J. Am. Chem. Soc. 145 (2023) 9965–9969.
[24] K. Wu, T.K. Ronson, P. Su, et al., Nat. Synth. 2 (2023) 789–797.
[25] D. Zhang, Q. Gan, A.J. Plajer, et al., J. Am. Chem. Soc. 144 (2022) 1106–1112.
[26] Y.Q. Zou, D. Zhang, T.K. Ronson, et al., J. Am. Chem. Soc. 143 (2021) 9009–9015.
[27] W.M. Bloch, S. Horiuchi, J.J. Holstein, et al., Chem. Sci. 14 (2023) 1524–1531.
[28] E. Benchimol, J. Tessarolo, G.H. Clever, Nat. Chem. 16 (2024) 13–21.
[29] K. Hema, A.B. Grommet, M.J. Białek, et al., J. Am. Chem. Soc. 145 (2023) 24755–24764.
[30] T.R. Schulte, J.J. Holstein, G.H. Clever, Angew. Chem. Int. Ed. 58 (2019) 5562–5566.
[31] S. Pullen, J. Tessarolo, G.H. Clever, Chem. Sci. 12 (2021) 7269–7293.
[32] T.Z. Xie, X. Wu, K.J. Endres, et al., J. Am. Chem. Soc. 139 (2017) 15652–15655.
[33] T.Z. Xie, K.J. Endres, Z. Guo, et al., J. Am. Chem. Soc. 138 (2016) 12344–12347.
[34] T.Z. Xie, K. Guo, Z. Guo, et al., Angew. Chem. Int. Ed. 54 (2015) 9224–9229.
[35] T.Z. Xie, S.Y. Liao, K. Guo, et al., J. Am. Chem. Soc. 136 (2014) 8165–8168.
[36] D. Chakraborty, N. Kaur, J. Sahoo, et al., J. Am. Chem. Soc. 146 (2024) 24901–24910.
[37] R. Banerjee, D. Chakraborty, P.S. Mukherjee, J. Am. Chem. Soc. 145 (2023) 7692–7711.
[38] J. Chen, Y.H. Huang, J. Yang, et al., J. Am. Chem. Soc. 146 (2024) 32738–32747.
[39] W. Yang, Q. Mo, Q.T. He, et al., Angew. Chem. Int. Ed. 63 (2024) e202406564.
[40] Y.L. Lai, M. Xie, X.C. Zhou, et al., Angew. Chem. Int. Ed. 63 (2024) e202402829.
[41] F. Yin, J. Yang, L.P. Zhou, et al., J. Am. Chem. Soc. 146 (2024) 7811–7821.
[42] S.P. Zheng, Y.W. Xu, P.Y. Su, et al., Chin. Chem. Lett. 35 (2024) 108477.
[43] Y. Ding, C. Shen, F. Gan, et al., Chin. Chem. Lett. 32 (2021) 3988–3992.
[44] D. Luo, B. Pan, J. Zhang, et al., Chin. Chem. Lett. 32 (2021) 1397–1399.
[45] Y.L. Lai, J. Su, L.X. Wu, et al., Chin. Chem. Lett. 35 (2024) 108326.
[46] R. Sarkar, T.Z. Xie, K.J. Endres, et al., J. Am. Chem. Soc. 142 (2020) 5526–5530.
[47] J. Wang, Z. Jiang, W. Liu, et al., Angew. Chem. Int. Ed. 62 (2023) e202214237.
[48] Q. Dong, F. Liu, J. Wang, et al., Angew. Chem. Int. Ed. 64 (2025) e202416327.
[49] Z. Jiang, Z. Wu, J. Wang, et al., Nano Res. 16 (2023) 9584–9590.
[50] F. Su, S. Zhang, Z. Chen, et al., J. Am. Chem. Soc. 144 (2022) 16559–16571.
[51] L. He, H.K. Hsu, L. Li, et al., Chem 8 (2022) 494–507.
[52] Y.S. Chen, E. Solel, Y.F. Huang, et al., Nat. Commun. 10 (2019) 3443.
[53] J. Shi, W. Xu, H. Yu, et al., J. Am. Chem. Soc. 145 (2023) 24081–24088.
[54] T. Wu, Z. Jiang, Q. Bai, et al., Chem 7 (2021) 2429–2441.
[55] D. Liu, M. Chen, K. Li, et al., J. Am. Chem. Soc. 142 (2020) 7987–7994.
[56] Z. Jiang, H. Zhao, J. Wang, et al., Chin. Chem. Lett. 34 (2023) 108334.
[57] T. Wu, Z. Jiang, X. Xue, et al., Chin. Chem. Lett. 32 (2021) 1911–1914.
[58] G. Wang, M. Chen, J. Wang, et al., J. Am. Chem. Soc. 142 (2020) 7690–7698.
[59] Z. Zhang, Y. Li, B. Song, et al., Nat. Chem. 12 (2020) 468–474.
[60] J. Wang, H. Zhao, M. Chen, et al., J. Am. Chem. Soc. 142 (2020) 21691–21701.
[61] Z. Li, Y. Li, Y. Zhao, et al., J. Am. Chem. Soc. 142 (2020) 6196–6205.
[62] Z. Jiang, B. Chen, H. Zhao, et al., J. Am. Chem. Soc. 146 (2024) 16721–16728.
[63] B. Song, Z. Zhang, K. Wang, et al., Angew. Chem. Int. Ed. 56 (2017) 5258–5262.
[64] X. Lang, W. Ma, Y. Zhao, et al., Chem. Eur. J. 18 (2012) 2624–2631.
[65] G.J. Chen, H.C. Ma, W.L. Xin, et al., Inorg. Chem. 56 (2017) 654–660.
[66] K. Wu, X.Y. Liu, P.W. Cheng, et al., J. Am. Chem. Soc. 145 (2023) 18931–18938.
[67] H. Hao, J.L. Shi, H. Xu, et al., Appl. Catal. B: Environ 246 (2019) 149–155.
[68] H. Yin, J. Yuan, J. Wang, et al., Energy Environ. Sci. 18 (2025) 2231–2242.
[69] E.M. Han, W.D. Yu, L.J. Li, et al., Chem. Commun. 57 (2021) 2792–2795.